Int. J. Electrochem. Sci., 9 **(2014)** 3602 - 3617

International Journal of
ELECTROCHEMICAL
SCIENCE
www.electrochemsci.org

Novel Conductive Gel Polymers based on Acrylates and Ionic Liquids

Martin Tosoni[1,*], *Michael Schulz*[2], *Thomas Hanemann*[1,2]

[1] Karlsruher Institut für Technologie (KIT), Institut für Angewandte Materialien - Werkstoffprozesstechnik, Hermann-von-Helmholtz-Platz 1, 76344 Eggenstein-Leopoldshafen, Germany
[2] Universität Freiburg, Institut für Mikrosystemtechnik, Georges-Köhler-Allee 102, 79110 Freiburg, Germany
[*]E-mail: martin.tosoni@kit.edu

Received: 14 February 2014 / *Accepted:* 3 March 2014 / *Published:* 14 April 2014

In this work, novel ionic gel conductive polymers were synthesised using thermally and UV-light induced polymerization. The gel polymers are based on poly(methyl methacrylate) (PMMA) containing ionic liquids (IL) and conductive salt (lithium bis(trifluoro-methanesulfonyl)imide, LiTFSI). Additional acrylates like 2-ethoxyethyl methacrylate (EEMA) and ethylene glycol dimethacrylate (EDMA) were used to modify and increase lithium mobility in these gel type networks. Electrochemical impedance spectroscopy was utilized to determine ionic conductivity and thermal analysis (DSC, TGA) to determine thermal behavior. Cell tests were performed as proof-of-principle studies for using gel polymer electrolytes in cell systems including electrode materials like $Li[Ni_{1/3}Mn_{1/3}Co_{1/3}]O_2$ (NMC), graphite (C) and lithium metal (Li).

Keywords: Gel polymer electrolytes, Ionic liquids, Poly(methyl methacrylate), Li-ion-batteries

1. INTRODUCTION

Gel polymer electrolyte films are frequently used as excellent substitutes for liquid electrolytes in lithium ion batteries, which help to improve safety and reliability [1]. An ideal GPE is characterized by high lithium ion mobility, flexible structure, low glass transition point and high thermal stability. Polyethylene oxide (PEO) has been established as material for gel polymer electrolytes (GPE) [2-8], but has some limitations such as low ionic conductivity at room temperature due to its tendency to crystallize below 60 °C [9-13]. Poly(methyl methacrylate) (PMMA) was first introduced as GPE-matrix by Feuillade [14]. Later poly(acrylonitrile)-poly(ethylene glycol diacrylate) blends were reported by Cho et al. [15]. PMMA side chain-modified acrylates offer new possibilities for

applications below 60 °C. The intention of side chain-modification was enabling enhanced lithium ion mobility due to polar atom groups in analogy to PEO. Here a lithium ion "hopping mechanism" seems to be possible. Since PMMA is a pure amorphous polymer, there are no crystalline phases, such as in PEO systems. Therefore, these are of particular interest for the development of new electrolytes. Other common gel polymer electrolytes are based on PVDF-HFP [16-20].

Ionic liquids (IL) have attracted remarkable interest for lithium ion batteries based on their beneficial properties such as non-volatility, non-flammability, a wide electrochemical window (ECW), and a high ionic conductivity [21-25].

Some ionic-liquid-based GPE have been examined for the use in further applications like capacitors and other battery types. [26-33]

In this work, we report novel syntheses and characterizations of gel polymer films based on acrylates and ionic liquids. These films consist of 1-methyl-1-propylpyrrolidinium bis(trifluoro-methanesulfonyl)imide (MPPyrrTFSI), the conductive salt lithium bis(trifluoro-methanesulfonyl)imide (LiTFSI) and various PMMA copolymers as polymer matrices. The polymerization was done by creating homogeneous mixtures of MPPyrrTFSI, LiTFSI, radical starter, acrylic resin (Plexit 55, Röhm) and acrylic compounds like 2-ethoxyethyl methacrylate (EEMA), poly(ethylene glycol) ethyl ether methacrylate (PEGEEM), ethylene glycol dimethacrylate (EDMA) and tri(ethylene glycol) dimethacrylate (TEGDMA). After inducing polymerization via heating or UV irradiation, homogeneous gel polymer electrolytes were obtained. A variety of characterization experiments, namely thermal analysis (DSC, TGA), size exclusion chromatography (SEC), cyclic voltammetry (CV), electrochemical impedance spectroscopy (EIS) and battery cycling tests have been carried out.

2. EXPERIMENTAL

2.1 Reagents

1-Methyl-1-propylpyrrolidinium bis(trifluoromethanesulfonyl) imide (MPPyrrTFSI, IoLiTec) and lithium bis(trifluoromethanesulfonyl)-imide (LiTFSI, IoLiTec) were dried at 110 °C by means of a continuous flow of dried air. Vinylene carbonate (VC, 97% Sigma-Aldrich), dilauroyl peroxide (Luperox 97%, Sigma-Aldrich), Plexit 55 acrylic resin (30% polymer in 70% methyl methacrylate, Röhm), acetone (Merck), poly(ethylene glycol) ethyl ether methacrylate (PEGEEM, M_n=246, Sigma-Aldrich), ethylene glycol dimethacrylate (EDMA, 98%, Sigma-Aldrich), 2-ethoxyethyl methacrylate (EEMA, 99%, Sigma-Aldrich), tri(ethylene glycol) dimethacrylate (TEGDMA, 95%, Sigma-Aldrich), Irgacure-1700 (Ciba Co.) and LP30 (1 M $LiPF_6$ in EC/DMC 1:1, Merck) were used as received.

2.2 Conductive acrylic polymers

2.2.1 Thermal synthesis route

The acrylate copolymers were prepared by thermally induced polymerization. Dilauryl

peroxide was used as radical initiator (0.5 wt% of total weight). First, the acrylic resin Plexit 55, the corresponding monomer or oligomer and dilauryl peroxide were homogeneously mixed using a high-performance disperser (Ultra Turrax, IKA). Then polymerization was started at a temperature of 80 °C. After a reaction time of 24 hours the temperature was raised to 90 °C and held for a further hour to allow residual monomer to react completely, resulting in a transparent solid bulk material. A mechanical comminution into a fine powder was done by using a cryogenic mill (6800 FREEZER/MILL, from SPEX CertiPrep). For gelation it was intended to dissolve the powder in a suitable solvent (acetone) and IL/conductive salt mixture was added. The solvent should have been quantitatively removed by vacuum extraction. This planed preparation failed because only few copolymers (like PMMA/PEEMA) were soluble in acetone, so another more suitable polymerization *in situ* method was developed using UV-radiation (2.2.2). All upcoming IL-GPE were prepared by employing this *in situ* procedure.

2.2.2 In situ gel preparation via UV polymerization

Since all components were added together at the same time, this process is called *in situ* gel preparation. It can be used for small experimental batches (e.g. UV-LED reactor) as well as for larger scales using industrial UV lamps. Plexit 55, acrylic monomers (e.g. EEMA, EDMA, etc.), IL, conductive salt, UV starter (Irgacure-1700) and a small amount of acetone as solvent were mixed and polymerization was started with UV light (24h, self-made UV reactor: 400 nm, 0.6 W). The volatile solvent is quantitatively removed by vacuum extraction from the resulting gel polymer (Fig. 1).

Figure 1. Photograph of IL-GPE in a teflon ring (Ø=12.7mm), PMMA/PEEMA 90:10 (UV *in situ*) (25wt%), MPPyrrTFSI, 0.3 M LiTFSI

2.3 Size exclusion chromatography (SEC)

SEC measurements were performed with a P100 pumping unit and a sample robot AS100 (Thermo Finnigan). The signals were detected by a refractive index analyser RI 71 (Showa Denko). Tetrahydrofuran (THF) was used as solvent and a polystyrene (PS)-gel column set (1x 100 Å, 1x 10^4 Å, 1x 10^3 Å , 2x 100 Å, Polymer Standards Service) was utilized (sample concentration: 1 mg/ml). Toluene was added (1 µl/ml) as internal standard and all data were corrected to this standard. The signal recording, calibration (with PMMA calibration samples from Polymer Standards Service) and analysis were done by the software WinGPC 7.2 (Polymer Standards Service).

2.4 Differential scanning calorimetry (DSC)

The polymers and gels were investigated by differential scanning calorimetry on their phase behaviour (DSC, Netzsch DSC 204 F1 Phoenix ®, Al crucible). Measurements were carried out from 30 to 550 °C at a heating rate of 10 K/min in air atmosphere.

2.5 Thermogravimetric analysis (TGA)

Thermogravimetric analysis (TGA) was performed using a thermal analysis balance NETZSCH STA 409 from 25 °C to 1000 °C under air flow (20 ml/min). The mass loss was evaluated between 25 °C and 1000 °C.

2.6 Conductivity

For conductivity measurements, a Swagelok-type cell design was used by placing two stainless steel cylinders (diameter 12.7 mm). The ionic conductivity is calculated from $\sigma = L/(A\ R_b)$, where A and L represent the free area and thickness between the stainless steel rods. R_b is the bulk resistance obtained from the EIS measurements in the frequency range from 1 Hz to 4 MHz with an AC amplitude of 100 mV. The ionic conductivity was calculated using the bulk impedance at the zero phase angle resistance. Impedance measurements were carried out using a Zahner Zennium electrochemical workstation. The setup was calibrated with a 0.1 M KCl solution with a conductivity of 11.6 ± 1.0 mS/cm (20 °C) corresponding to Hamann et al. [34]. Conductivity measurements of polymers and gel polymer films were performed by sandwiching the films between two stainless steel rods.

2.7 Cyclic voltammetry (CV)

The electrochemical windows of the gel polymer films were determined using cyclic voltammetric (CV) technique in a symmetric standard two electrode Swagelok cell, SS/GPE/SS (SS: stainless steel). The potential was scanned between –4 V to 4 V at 10 mV/s for 5 CV cycles.

2.8 Cell cycling tests

All cells were assembled in an argon-filled glove box (oxygen and water levels below 0.5 ppm, MBraun GmbH) using CR2032 coin cells with following parameters: diameter = 20 mm, thickness = 3.2 mm, electrode dimensions: Ø = 15 mm, case material: stainless steel V2A and V4A. Glass microfiber filters from Whatman (GF/B type, Ø = 16 mm) were deployed. The GPEs were applied with a pipette (300 µl per cell) after the GPE were heated up to 60 °C to become viscous fluids. At this temperature the GPE was fluid enough to be applied using a pipette and it is further ensured that the LiTFSI-salt does not yet decompose. The closure of the coin cells took place with a constant pressure of 75 bar. Different electrodes of standard materials, such as graphite, $Li[Ni_{1/3}Mn_{1/3}Co_{1/3}]O_2$ (NMC) and Li metal foil (Alfa Aesar, 0.75 mm thickness) were used. The electrodes were based on graphite and NMC, respectively, with a content of approx. 90 % of active material.

3. RESULTS AND DISCUSSION

3.1 Size exclusion chromatography of pure polymers

The following pure acrylate polymers were characterized regarding their molecular weights using size exclusion chromatography (Tab.1).

Table 1. Number average molecular weight M_n, weight average molecular weight M_w, average molecular weight M_z of GPE and polydispersity index PDI

polymer	M_n [g/mol]	M_w [g/mol]	M_z [g/mol]	PDI
PMMA/PEEMA 90:10	12 500	4 090 000	4.83×10^{10}	327
PMMA/PEGEEMA 90:10	9 510	415 000	2.90×10^{10}	43.7
PMMA/PTEGDMA 90:10	6 190	6 500 000	4.84×10^{10}	1 050
PMMA/PEDMA 90:10	18 700	3 300 000	6.31×10^{10}	177
PMMA/PEEMA 90:10 (UV)	5 650	1 010 000	6.39×10^{10}	179
PMMA (pure Plexit 55, UV)	5 900	827 000	1.48×10^{8}	140
PMMA (pure Plexit 55, th.)	98 500	1 850 000	8.02×10^{10}	18.8
PMMA/MMA (pure Plexit 55, resin)	4 160	99 000	1.30×10^{5}	23.8

Polymers obtained from the UV-irradition-process provide shorter chain lengths, e.g. PMMA/PEEMA (UV): M_n= 5 650 g/mol and M_w= 1 010 000 g/mol. Thermal polymerization of

PMMA/PEEMA generates polymer chains with M_n= 12 500 g/mol and M_w= 4 090 000 g/mol. This is also true for pure PMMA (Plexit 55), which showed higher molecular weights M_n and M_w, when using the thermal synthesis route. PMMA/PEEMA copolymers with UV light polymerization showed narrow distributed polymers, which can be seen in different values of polydispersity PDI=M_w/M_n ($PDI_{thermal}$=327, PDI_{UV}=179). In contrast to these results the thermal polymerization of PMMA leaded to a PDI of 18.8, while a PDI value of 140 was determined for UV polymerization.

3.2 Differential scanning calorimetry (DSC)

3.2.1 DSC measurements of pure polymers

All samples first showed endothermic areas, which correspond to depolymerization and degradation effects (Fig.2). This is followed by endothermic decompositions at higher temperatures, due to oxidation processes in air atmosphere (~350 °C). PMMA/PEEMA (thermic polymerization) and PMMA/PEGEEMA start to decompose at 200 °C. Other polymers had higher degradation temperatures like PMMA/PEEMA (UV-light polymerization) (240 °C), PMMA/PEDMA (250 °C) and PMMA/PTEGDMA (220 °C). Small distinctive glass transition ranges were detected for all probes and around 90-100 °C. Thus, a wide operating temperature from room temperature up to 200 °C is ensured.

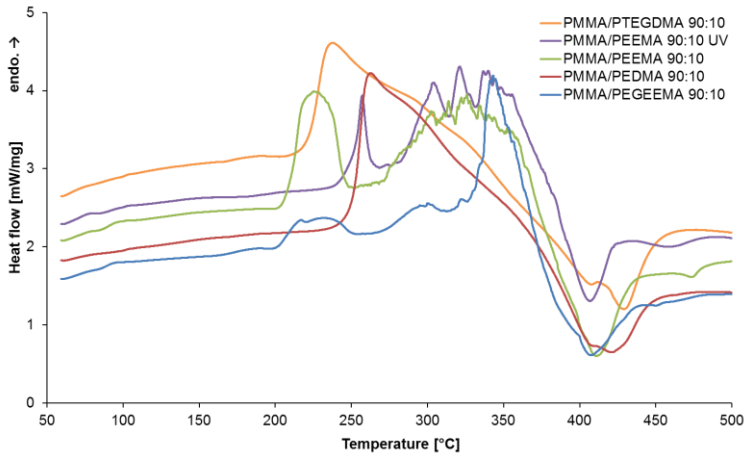

Figure 2. Differential scanning calorimetry of pure polymers at 10 K/min, air atmosphere

3.2.2 DSC measurements of IL-GPE

In Fig. 3 a DSC curve of an IL-GPE is shown. The PMMA/PEEMA-gel showed even a higher thermal stability in comparison to the pure PMMA/PEEMA polymer. No degradation effects were detected until 260 °C, which offers a broad field for applications. A large exothermic material conversion started around 400 °C, which corresponds to the decomposition of IL and conductive salt. This fact supports the passive safety of the system by using IL and TFSI-Anions.

The IL probably acts as plasticizer for the acrylic polymer, because no glass transitions can be detected like for the pure PMMA/PEEMA polymers. Pandey and Hashmi found a similar temperature range of use for PVDF-HFP-type gels (up to 250 °C) [33]. In contrast to PVDF-HFP-GPE no melting peak was found. These endothermic peaks in PVDF-HFP-systems typically appear at ~110-140 °C [17] due to small crystalline domains in PVDF-HFP-GPE matrices.

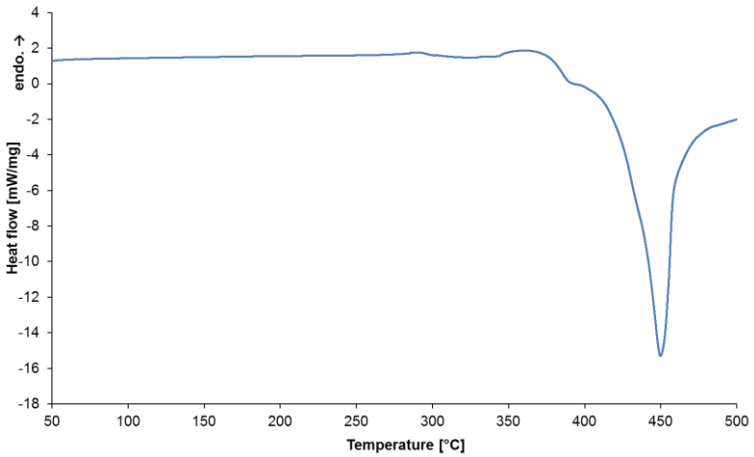

Figure 3. Differential scanning calorimetry of IL-GPE: PMMA/PEEMA 90:10 (UV *in situ*) (25wt%), MPPyrrTFSI, 0.3 M LiTFSI, air atmosphere

3.3 Thermogravimetric analysis (TGA)

3.3.1 TGA measurements of pure polymers

Fig. 4 shows TGA results for some pure polymers. All samples show almost no loss in weight up to 200 °C (2% or less). A specialty of IL-GPE is the non-volatility which was proven via DSC and TGA. Above 250 °C a strong mass loss is observed, which corresponds to an endothermic decomposition (checked by appropriate DSC investigations, Chap. 3.2).

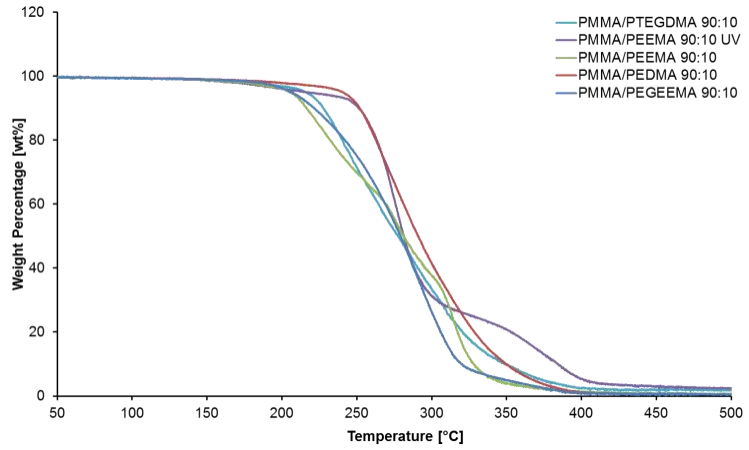

Figure 4. Thermogravimetric analysis (TGA) of pure polymers, air atmosphere

3.3.2 TGA measurements of IL-GPE

As proven by DSC experiments, the presence of IL leads to a greater thermal stability of the resulting gel polymer. This could also be verified by TGA measurements (Fig. 5). While pure acrylic polymers start to decompose around 200 °C, PMMA/PEEMA gels are stable up to 270 ° C.

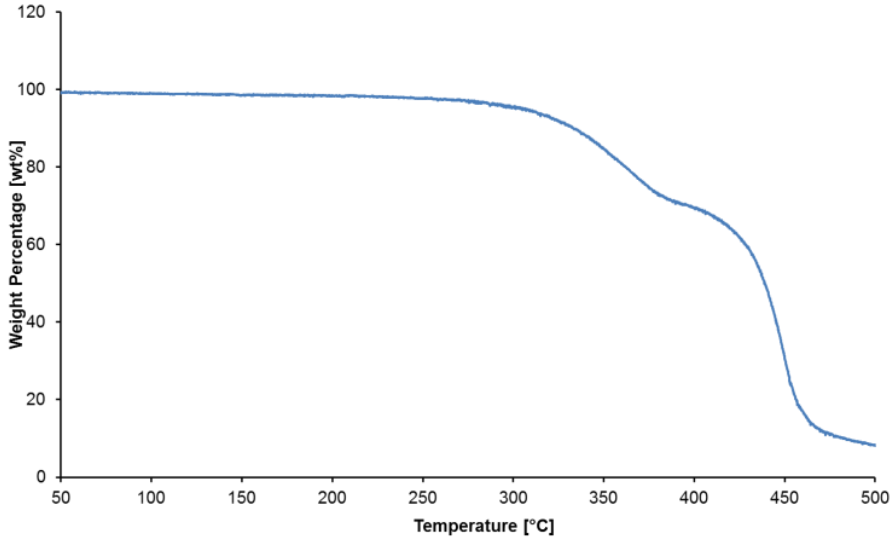

Figure 5. Thermogravimetric analysis of IL-GPE: PMMA/PEEMA 90:10 (UV *in situ*) (25wt%), MPPyrrTFSI, 0.3 M LiTFSI, air atmosphere

3.4 Electrochemical Properties

3.4.1 Conductivities of pure polymers

Fig. 6 shows conductivities of the pure polymers (thermal and UV-light) obtained from electrochemical impedance spectroscopy. Different PMMA to copolymer (PEEMA, PEGEEMA, PTEGDMA, PEDMA) ratios were screened. In general it was found, that lower amounts of PMMA increase conductivity of the resulting polymers. Therefore all 90:10-polymers showed higher conductivities compared to 93:7-polymers for instance. This can be explained by the increased quantity of polar copolymer and the effect is similar to the one observed in PEO-systems [6, 7]. The highest conductivity was found for PMMA/PEEMA 90:10, which reached 4.87 x 10^{-9} mS/cm (for comparison pure PEO-systems (60 °C): 10^{-10}–10^{-8} mS/cm) [6, 7]. The low conductivities can be explained by the absence of Li salts and swelling agents, which were added in the alternative *in situ* gel preparation method (Chap. 2.2.2 and 3.4.2).

UV-light polymerization leads to slightly higher conductive polymers than the thermal polymerization (PMMA/PEEMA: 4.87 x 10^{-9} mS/cm vs. 2.33 x 10^{-9} mS/cm). The shorter chain lengths offer greater flexibilities, which cause an increase in conductivities.

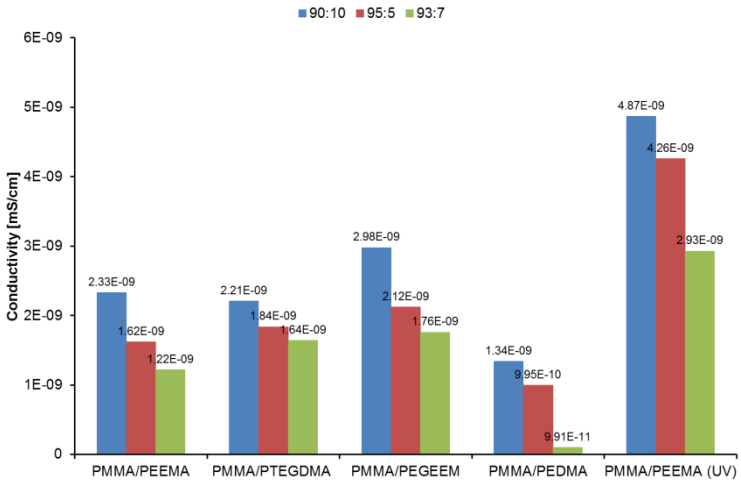

Figure 6. Conductivities of pure polymers

3.4.2 Ionic conductivities of IL-GPE (UV in situ gel preparation)

Since thermal and UV-light polymers were insoluble in IL+solvent when prepared first, the in situ gel preparation method using UV-light was utilized to create IL-GPE. Some ionic conductivities of IL-gel polymer electrolytes are listed in Tab. 2. The investigated films had a concentration of 0.3 M LiTFSI and a polymer content of 25 wt%. The addition of IL and conductive salt increases conductivity strongly to 0.77 mS/cm (IL-GPE) (for comparison: LP30 from Merck = 1 M $LiPF_6$ in EC/DMC: 30 mS/cm). Typical GPE based on PVDF-HFP have an ionic conductivity around 2-2.8 mS/cm [16]; with the addition of IL the conductivity reaches 0.27 mS/cm [17] up to 5.8 mS/cm [18]. PEO polymer electrolytes offer conductivities of 0.1 mS/cm at 60 °C [13]. PEO-systems with Li salts: 10^{-5}–10^{-1} mS/cm [6, 7, 13]

Monoacrylic systems like PMMA/PEEMA and PMMA/PEGEEMA showed conductivities of 0.77 mS/cm and 0.75 mS/cm. A slight decrease in conductivity has been observed due to higher cross linked diacrylates PMMA/PTEGDMA (0.45 mS/cm) and PMMA/PEDMA (0.40 mS/cm) resulting in a less flexible network.

Table 2. Ionic conductivities of IL-GPE (UV *in situ*) at 25 °C

polymer	IL	conductive salt concentration	polymer content	σ [mS/cm]
PMMA/PEEMA 90:10 (UV *in situ*)	MPPyrrTFSI	0.3 M LiTFSI	25wt%	0.77
PMMA/PEGEEMA 90:10 (UV *in situ*)	MPPyrrTFSI	0.3 M LiTFSI	25wt%	0.75
PMMA/PTEGDMA 90:10 (UV *in situ*)	MPPyrrTFSI	0.3 M LiTFSI	25wt%	0.45
PMMA/PEDMA 90:10 (UV *in situ*)	MPPyrrTFSI	0.3 M LiTFSI	25wt%	0.40

A higher concentration of 1 M LiTFSI results in lower conductivities of gel polymer films (Tab. 3). This can be explained with the possible increase of viscosity and higher probability of aggregate formations when more Li-salt is. The ionic conductivities cover a range from 0.19 to 0.60 mS/cm for GPE systems containing 1 M LiTFSI.

Although the addition of more conductive salt leads to lower conductivities, this is necessary to increase performance in Li/NMC- and NMC/C-cells (Chap. 3.4.5).

Table 3. Ionic conductivities of IL-GPE (UV *in situ*) at 25 °C

polymer	IL	conductive salt concentration	polymer content	σ [mS/cm]
PMMA/PEEMA 90:10 (UV *in situ*)	MPPyrrTFSI	1 M LiTFSI	25wt%	0.60
PMMA/PEGEEMA 90:10 (UV *in situ*)	MPPyrrTFSI	1 M LiTFSI	25wt%	0.54
PMMA/PTEGDMA 90:10 (UV *in situ*)	MPPyrrTFSI	1 M LiTFSI	25wt%	0.21
PMMA/PEDMA 90:10 (UV *in situ*)	MPPyrrTFSI	1 M LiTFSI	25wt%	0.19

Lower conductivities are observed, if more polymer is added, resulting in harder and more stable gels (Tab. 4). For a PMMA/PEEMA-GPE a conductivity of 0.09 mS/cm was determined with a polymer content of 50wt%.

Table 4. Ionic conductivities of IL-GPE (UV *in situ*) at 25 °C

polymer	IL	conductive salt concentration	polymer content	σ [mS/cm]
PMMA/PEEMA 90:10 (UV *in situ*)	MPPyrrTFSI	0.3 M LiTFSI	25wt%	0.77
PMMA/PEEMA 90:10 (UV *in situ*)	MPPyrrTFSI	0.3 M LiTFSI	33wt%	0.24
PMMA/PEEMA 90:10 (UV *in situ*)	MPPyrrTFSI	0.3 M LiTFSI	50wt%	0.09

In Tab. 5 the temperature dependence of a PMMA/PEEMA gel polymer electrolyte is presented from 20 to 35 °C. As expected for typical ionic liquid systems, the conductivity increases on higher temperatures. At 35 °C the conductivity is slightly below 1 mS/cm.

Table 5. Ionic conductivities of IL-GPE (UV *in situ*), 25wt% at different temperatures varying from 20 to 35 °C

polymer	IL	conductive salt concentration	temp [°C]	σ [mS/cm]
PMMA/PEEMA 90:10 (UV *in situ*)	MPPyrrTFSI	0.3 M LiTFSI	20	0.65
PMMA/PEEMA 90:10 (UV *in situ*)	MPPyrrTFSI	0.3 M LiTFSI	25	0.77
PMMA/PEEMA 90:10 (UV *in situ*)	MPPyrrTFSI	0.3 M LiTFSI	30	0.86
PMMA/PEEMA 90:10 (UV *in situ*)	MPPyrrTFSI	0.3 M LiTFSI	35	0.98

3.4.3 Cyclic voltammetry (CV) of IL-GPE (UV in situ gel pre-paration)

To investigate the electrochemical stability of the IL-gel polymer electrolyte, cyclic voltammetry was applied to these systems. CV curves were recorded using symmetrical cells (SS/IL-GPE/SS). A typical CV curve for an IL-GPE consisting of PMMA/PEEMA 90:10 (UV *in situ*) (25wt%), MPPyrrTFSI, 0.3 M LiTFSI is shown in Fig. 7.

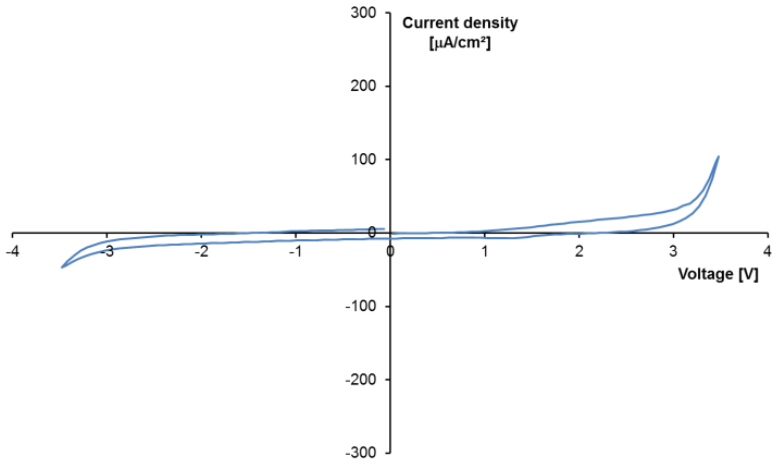

Figure 7. Cyclic voltammetry of a SS/IL-GPE/SS-cell at 25 °C, PMMA/PEEMA 90:10 (UV *in situ*) (25wt%), MPPyrrTFSI, 0.3 M LiTFSI

From these measurements, the electrochemical windows (ECW) in Tab. 6 were graphically determined by extrapolation (using a method in analogy to DIN 51005). The intersections between extrapolated baselines and tangents of the rising flanks were used as onset and offset points.

Table 6. Cyclic voltammetry (CV) of IL-GPE (UV) at 25 °C

polymer	IL	conductive salt concentration	polymer content	ECW [V]
PMMA/PEEMA 90:10 (UV *in situ*)	MPPyrrTFSI	0,3 M LiTFSI	25wt%	5.5
PMMA/PEGEEMA 90:10 (UV *in situ*)	MPPyrrTFSI	0,3 M LiTFSI	25wt%	5.5
PMMA/PTEGDMA 90:10 (UV *in situ*)	MPPyrrTFSI	0,3 M LiTFSI	25wt%	5.4
PMMA/PEDMA 90:10 (UV *in situ*)	MPPyrrTFSI	0,3 M LiTFSI	25wt%	5.4

The electrochemical stabilities of all examinated IL-GPE listed in Tab. 6 are quite similar and showed stabilities up to 5.5 V. A great difference between various polymers like PMMA/PEEMA, PMMA/PEGEEMA, PMMA/PTEGDMA and PMMA/PEDMA was not observed. So, the ECW is mainly depending upon the IL used and conductive salt.

3.4.5 Battery cycling tests of IL-GPE (UV in situ gel preparation)

The acrylic GPE made of PMMA/PEEMA 90:10 (UV) (25wt% polymer content), MPPyrrTFSI, LiTFSI, VC (10wt%) were successfully tested in coin cell batteries. Vinylene carbonate (VC) as SEI (solid electrolyte interphase) building agent is not necessary needed for Li/NMC-half cells, but was used to obtain comparable data to NMC/graphite-full cells.

Two different amounts of LiTFSI (0.3 and 1 M) were used. The galvanostatic charging/discharging curves of Li/NMC-half cells are shown in Fig. 8. It has been shown, that cells with 1 M conductive salt showed much better performances, even though conductivities are lower (Chap. 3.4.2). At charging/discharging rates of C/50, a gravimetric capacity of 140 mAh/g was achieved for these systems, whereas only 100 mAh/g were measured for cells with concentrations of 0.3 M LiTFSI. A possible reason can be found in the structure of the gel: Polar O atoms from acrylic groups may block some Li ions and decrease charge transport. Therefore a higher Li ion concentration is advantageous.

For NMC/graphite-full cells it is important to form a stable SEI-layer to allow reversible charge/discharge cycles. It must be ensured that no IL cations are intercalated into the graphite lattice instead of Li ions. This was done by adding vinylene carbonate (VC) as SEI builder in the GPE. The unusual high amout of 10wt% VC is needed because the SEI is formed only by VC itself. In common carbonate-based mixtures like LP30 (1 M $LiPF_6$ in EC/DMC 1:1, Merck) these carbonates are integrated in the SEI formation process.

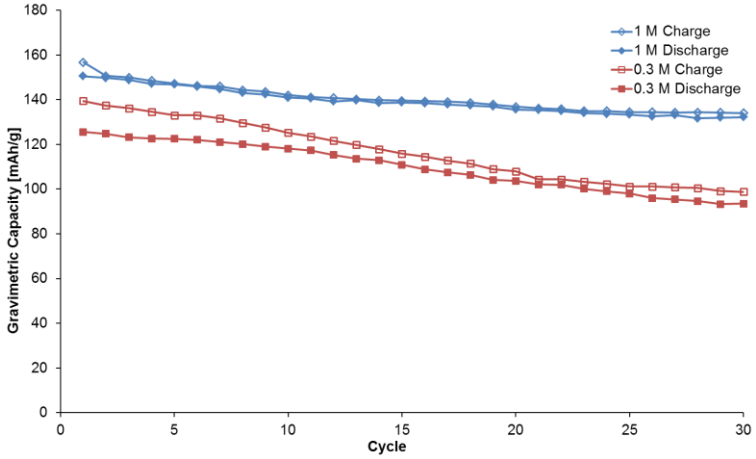

Figure 8. Battery cycling tests of Li/IL-GPE/NMC at 25 °C, C/50 with 0.3 and 1 M LiTFSI, 10wt% VC

By this means a suitable GPE for graphite electrodes was obtained. The corresponding test cells had a discharge capacity of 106 mAh/g (1 M LiTFSI) and 72 mAh/g (0.3 M LiTFSI respectively) at C/50 (Fig. 9).

The investigated GPE only performed well at low charging rates (i.e. C/50-C/30). In order to achieve higher C-rates, the addition of organic compounds like ethylene carbonate (EC), propylene carbonate (PC) and dimethyl carbonate (DMC) is promising.

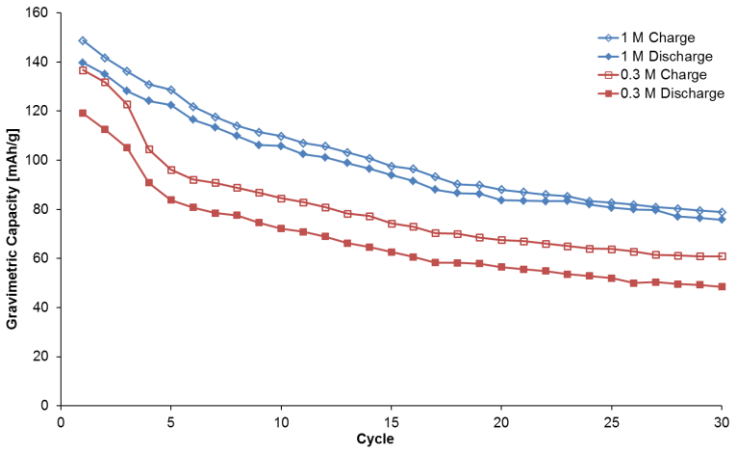

Figure 9. Battery cycling tests of NMC/IL-GPE (UV)/graphite at 25 °C, C/50 with 0.3 and 1 M LiTFSI, 10wt% VC

If temperature is increased from 25 to 40 °C the test cells performed better and showed smaller fading in capacity after 30 cycles at 40 °C (Fig. 10). This can be explained by higher conductivities of IL-gel polymer films, which result in better mobilities of Li ions. At higher temperatures the viscosity decreases, because of reduced ionic attractions between ions and the decrease of Van der Waals forces between polymer chains and alkyl chains of IL cations.

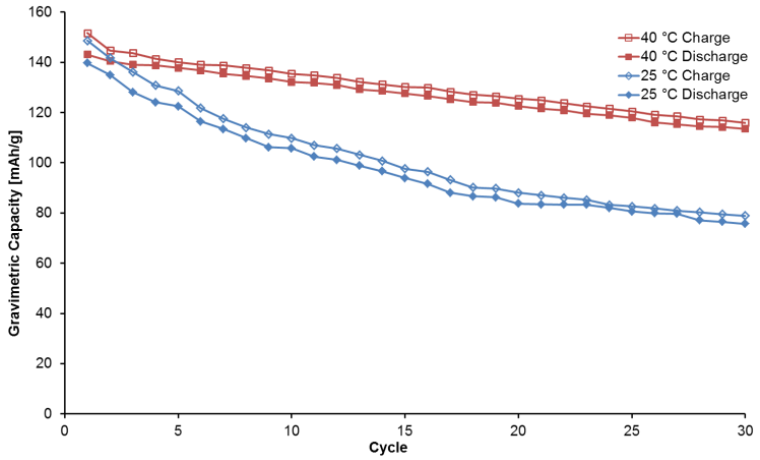

Figure 10. Battery cycling tests of NMC/IL-GPE (UV)/graphite, 1 M LiTFSI at 25 and 40 °C, C/50, 10wt% VC

To determine self-discharge, further tests were carried out and presented in Fig. 11 for fully charged cells. The IL-GPE cell had a slightly lower self-discharge of 12 mAh/g (~8%) than a NMC/LP30/graphite-reference cell, which had loss in capacity of 18 mAh/g (~12%) per month at 25 °C.

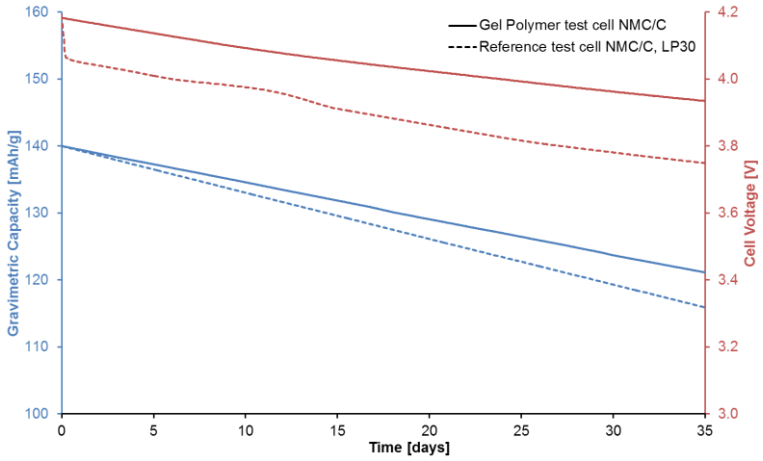

Figure 11. Voltage loss and capacity loss of NMC/IL-GPE (UV)/graphite- and NMC/LP30/C-test cells at 25 °C

This is close to the values given for commercial lithium ion batteries, which are indicated with a typical self-discharge of 5-10%/month [35, 36]. A possible explanation could be the better attachment of the SEI on the graphite surface due to the gel polymer network. Therefore less Li ions could deintercalate from the graphite pattern. Noteworthy is the low voltage drop at the beginning when using GPE in contrast to the high voltage drop of ~0.2 V with LP30 in cells.

4. CONCLUSIONS

GPE based on acrylates were synthesized successfully via *in situ* preparation. Different monoacrylic GPE like PMMA/PEEMA and PMMA/PEGEEMA showed conductivities around 0.75 mS/cm. Diacrylic polymers like PMMA/PTEGDMA and PMMA/PEDMA result in lower ionic conductivities (~0.4 mS/cm) for the corresponding gels.

When using IL in gels, only the UV *in situ* process is suitable; otherwise large insoluble polymers were generated. PMMA/ PEEMA-IL-GPE work well in Li/NMC- and NMC/C-cells and enable reversible cycles at lower charging rates (C/50-C/30). After 30 cycles the discharge capacities were 132 mAh/g (92% of initial discharge capacity) for Li/NMC-systems and 76 mAh/g (54% of initial discharge capacity) for NMC/C-full cells. Additional carbonates like EC and PC are expected to increase charging rates and should be investigated in further studies, although this might reduce thermal stability of the electrolytes.

ACKNOWLEDGEMENTS

We acknowledge Thomas Schubert and Maria Ahrens (IoLiTec Ionic Liquids Technologies GmbH) for kindly providing the ionic liquid. Further we like to thank Uwe Gleissner (IMTEK, University of Freiburg) for performing TGA measurements and Andreas Hofmann for helpful discussions. We acknowledge support by Deutsche Forschungsgemeinschaft and Open Access Publishing Fund of Karlsruhe Institute of Technology.

References

1. A. M. Stephan, *European Polymer Journal*, 42 (2006) 21–42.
2. W. Wieczorek, A. Zalewska, D. Raducha, F. Florjanczyk, J. R. Stevens, A. Ferry, P. Jacobsson, *Macromolecules*, 29 (1996) 143–147.
3. F. Croce, G. B. Appetecchi, L. Perci, B. Scrosati, *Nature*, 394 (1998) 456–458.
4. W. Wieczorek, J.R. Steven, Z. Florjanczyk, *Solid State Ionics*, 85 (1996) 67–72.
5. Q. Li, Y. Takeda, N. Imanish, J. Yang, Y. K. Sun, *J. Power Sources*, 97–98 (2001) 795–797.
6. Q. Li, N. Imanishi, A. Hirano, Y. Takeda, O. Yamamoto, *J. Power Sources*, 110 (2002) 38–45.
7. Q. Li, T. Itoh, N. Imanishi, A. Hirano, Y. Takeda, O. Yamamoto, *State Ionics*, 159 (2003) 97–109.
8. G. B. Appetecchi, J. Hassoun, B. Scrosati, F. Croce, F. Cassel, M. Salomon, *J. Power Sources*, 124 (2003) 246–253.
9. M. Armand, *Solid State Ionics*, 9–10 (1983) 745–754.
10. P. G. Bruce, *Electrochim Acta*, 40 (1995) 2077–2085.
11. D. E. Fenton, J. M. Parker, P. V. Wright, *Polymer*, 14 (1973) 589–590.
12. G. B. Appetecchi, F. Croce, L. Persi, F. Ronci, B. Scrosati, *J. Electrochem. Soc.*, 147 (2000) 4448–4452.
13. T. Caruso, S. Capoleoni, E. Cazzanelli, R. G. Agostino, P. Villano, S. Passerini, *Ionics*, 8 (2002) 36–43.
14. G. Feuillade, P. Perche, *J. Appl. Electrochem.*, 5 (1975) 63–69.
15. B.-W. Cho, D. H. Kim, H.-W.Lee, B.-K. Na, *Korean J. Chem. Eng.*, 24 (2007) 1037–1041.
16. W. Xiao, X. Li, Z. Wang, H. Guo, Y. Li, B. Yang, *Iran Polym. J.*, 21 (2012) 755–761.
17. H. Ye, J. Huang, J. J. Xu, A. Khalfan, S. G. Greenbaum, *J. Electrochem. Soc.*, 154 (2007) A1048–A1057.
18. J. Fuller, A. C. Breda, R. T. Carlin, *J. Electrochem. Soc.*, 144 (1997) L67–L70.

19. M.-K. Song, Y.-T. Kim, Y. T. Kim, B. W. Cho, B. N. Popov, H.-W. Rhee, *J. Electrochem. Soc.*, 150 (2003) A439–A444.
20. S. Kataria, S. K. Chaurasia, R. K. Singh, S. Chandra, *J. Phys. Chem. B*, 117 (2013) 897–906.
21. T. Sato, T. Maruo, S. Marokane, K. Takagi, *J. Power Sources*, 138 (2004) 253–261.
22. P. Wasserscheid, T. Welton, *Ionic Liquids in Synthesis*, Wiley-VCH: Weinheim (2003).
23. J. D. Holbery, K. R. Seddon, *Clean Prod. Proc.*, 1 (1999) 223.
24. R. D. Rogers, K. R. Seddon, (Eds.). *Ionic Liquids: Industrial Applications for Green Chemistry (ACS Symposium Series)*, American Chemical Society, ISBN 0-8412-3789-1, Washington DC., USA (2001).
25. J. S. Wilkes, *J. Mol. Catal.* 214 (2004) 11.
26. G. P. Pandey, Y. Kumar, S. A. Hashmi, *Indian J. Chem*, 49A (2010) 743–751.
27. M. Morita, T. Shirai, N. Yoshimoto, M. Ishikawa, *J. Power Sources*, 139 (2005) 351–355.
28. S. S. Sekhon, J. S. Park, E. Cho, Y. G. Yoon and C. S. Kim, K. Yamada, *J. Mater. Chem.*, 16 (2006) 2256–2265.
29. K.-S. Kim, S.-Y. Park, S. Choi, H. Lee, *J. Power Sources*, 155 (2006) 385–390.
30. W. Lu, K. Henry, C. Turchi, J. Pellegrino, *J. Electrochem. Soc.*, 155 (2008) A361–A367.
31. H. Ohno (Ed.), *Electrochemical Aspects of Ionic Liquids*, Wiley Interscience, New Jersey (2005).
32. C.S. Brazel, R. D. Rogers (Eds.), *Ionic Liquids in Polymer Systems, ACS Symposium Series 913*, American Chemical Society, Washington, DC (2005).
33. G. P. Pandey, S. A. Hashmi, *J. Power Sources*, 187 (2009) 627–634.
34. S. D. Hamann, M. Linton, *Trans. Faraday Soc.*, 65 (1969) 2186–2196.
35. H. Abe, T. Murai, K. Zaghib, *J. Power Sources*, 77 (1999) 110–115.
36. Manufacturer information in Technical Handbook from Sony, http://www.sony.com.cn/products/ed/battery/download.pdf (accessed 27. November 2013).